Available online at www.sciencedirect.com
ScienceDirect
Trans. Nonferrous Met. Soc. China 24(2014) 2282−2288
Transactions of Nonferrous Metals Society of China
www.tnmsc.cn

Effects of external stress aging on morphology and precipitation behavior of θ'' phase in Al−Cu alloy

Shang FU[1,2], Dan-qing YI[1,2], Hui-qun LIU[1,2], Yong JIANG[1,2], Bin WANG[1,2], Zhan HU[1,2]

1. School of Materials Science and Engineering, Central South University, Changsha 410083, China;
2. Key Lab of Nonferrous Materials (Ministry of Education), Central South University, Changsha 410083, China

Received 17 October 2013; accepted 3 April 2014

Abstract: The exposure of Al−5Cu alloy to an external stress with normal aging was carried out. The effects of external stress-aging on the morphology and precipitation behavior of θ'' phase were investigated by transmission electron microscopy (TEM), differential scanning calorimetry (DSC) and first principle calculation. The size of the θ'' phase precipitated plates in stress-aging (453 K, 6 h, 50 MPa) is 19.83 nm, which is smaller than that of those present (28.79 nm) in stress-free aging (453 K, 6 h). The precipitation process of θ'' phase is accelerated by loading external stress aging according to the analysis of DSC results. The apparent activation energy for the external stress-aging is 10% lower than the stress-free one. The first principle calculation results show that the external stress makes a decrease of 6% in the interface energy. The effects of the stress on aging process of the alloy are discussed on the basis of the classical theory. The external stress changes the morphology and precipitation behavior of θ'' phase because the critical nucleation energy is decreased by 19% under stress aging.

Key words: Al−Cu alloy; stress aging; morphology; precipitation behavior; first principle calculation; interface energy

1 Introduction

Precipitation strengthening via aging treatment is an important technique of enhancing the mechanical properties of age-hardenable aluminum alloys [1,2]. And the age-hardening response is mainly dominated by the precipitation behavior and the morphology of the meta-stable and stable precipitation phase [3]. As a typical type of age-hardenable aluminum alloy, 2xxx series Al−Cu alloy presents one of the most famous examples with the aging precipitation sequence (supersaturate solid solution−G.P. zone−θ'' phase−θ' phase−θ phase) [4,5]. And the θ'' phase is considered to be the first independent precipitation phase [6]. The previous works were focused on the optimization of the age-hardening response by changing the aging processing parameters and the alloy composition [7−10].

A few yeas ago, a novel external stress aging combing the external stress-field and traditional artificial aging was conducted into the age-hardenable alloy to improve the mechanical properties and the process of integral manufacture [11]. The precipitation phase morphologies of the super-alloy [12] and the zircaloy [13] were reported under external stress aging. HOSFORD and AGRAWAL [14] firstly introduced this technique into the processing of aluminum alloy and CHEN et al [15] found the microstructure of the precipitation phase existing to be anisotropic or stress-orientation effect. ZHU and STARKE [16] considered that this stress-oriented phenomenon depended on the alloy composition, aging parameters and the stress level. The possible explanations [15,16] of this phenomenon were the atomic diffusion and the precipitation/matrix lattice misfits. However, these explanations were not fully accepted since the explanations cannot satisfy all the reported results.

Generally, the energy of matrix and interface influences significantly the precipitation nucleation−growth behavior according to the classical transformation theory. But the hypothesis explanations mentioned above have not still given a clear description for the interface energy between precipitation phase and matrix under external stress because the evaluation of the

Foundation item: Project (2012CB619506) supported by the National Basic Research Program of China; Project (51071177) supported by the National Natural Science Foundation of China
Corresponding author: Dan-qing YI; Tel: +86-731-88830263; E-mail: yioffice@csu.edu.cn
DOI: 10.1016/S1003-6326(14)63345-8

interface energetic would be a challenge for the experimentalists. The first principle calculation is a useful method to investigate the energetic properties on the bulk material and interface between the secondary phase and matrix [17].

The aims in this work are to investigate the precipitation behavior and morphology of the θ'' phase under different external stress levels by DSC and TEM characterization methods. The effect of potential change of external stress on the interface energy and the critical nucleation energy is assessed by the first principle calculation based strategy according to the classical nucleation theory.

2 Experimental and computational method

The material used in this study was an Al−Cu alloy melted by induction furnace. The chemical composition of the alloy is listed in Table 1.

Table 1 Chemical composition of nominal Al−5Cu alloy (mass fraction, %)

Cu	Mg	Mn	Fe	Si	Zn	Al
4.99	0.01	0.008	0.01	0.026	0.012	Bal.

The ingots of the alloy were broken-down and rolled to sheets with the thickness of 2 mm. The sheets were solution heat treated at 773 K for 1 h, followed by water-quenching, and the sheets were then subjected to the external stress aging. The temperature for the external stress aging was determined as 453 K and the external stress levels were 0, 50 MPa (50 MPa was in the elastic load period according to the stress−strain curve yet). Hardness measurement was applied to determining the peak-aging time for each aging condition. The load for the hardness measurement was 1500 g. The TEM specimens of 3 mm in diameter were electro-polished with 30% nitric acid and 70% methanol solution at 253 K. TEM observation was performed on FEI Tecnai G^2 20 transmission electron microscope operated at 200 kV. Differential scanning calorimetry (DSC, NETZSCH DSC 200 F3) was performed on the specimens to investigate the transformation temperature and the θ'' phase precipitation behavior under different heat rates 10, 15, and 20 K/min. The first principle calculation was applied to determining the interface energy between Al matrix and the θ'' phase. All these calculations (including the bulk property optimization, the activity of Cu in Al under stress/strain and the interface energy as mentioned above) were determined by the Vienna ab initio simulation package (VASP) [18]. The parameter of the *K*-point mesh was followed by the energy convergent principle. The interface model (including a 12Å vacuum layer) is schematically shown in Fig. 1.

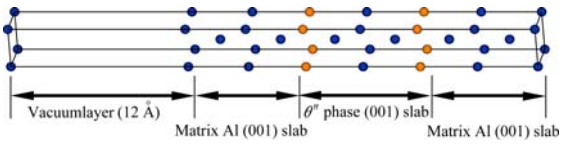

Fig. 1 Al matrix/precipitation θ'' phase interface model

3 Results and discussion

3.1 Age-hardening response and morphology of precipitation under external stress

The hardness versus aging−time curves under different external stress levels are exhibited in Fig. 2. The peak-aging time is 6 h from the curves and it shows that the peak-aging time is irrelevant with the external stress 50 MPa since it is in the elastic stress range which would only produce a strain at 0.006. During the under-age period, the hardness values of all different external stress levels samples are improved dramatically since the amount of the meta-stable phase precipitated from the supersaturated solid solution. Additionally, the major precipitation phase in this period is θ'' phase (the nominal composition of the θ'' phase is Al_3Cu) according to the 453 K aging temperature. Meanwhile, the higher external stress-level sample had the higher hardness compared with 0 stress level (or stress-free aging). It means that the external stress makes the precipitation response more significantly and rapidly. The traditional precipitation strengthening view holds that the strong precipitation response is caused by the decreasing of the precipitation barrier energy [5]. Generally speaking, the external stress is considered to be a sort of energy source to have an impact on the aging processing response.

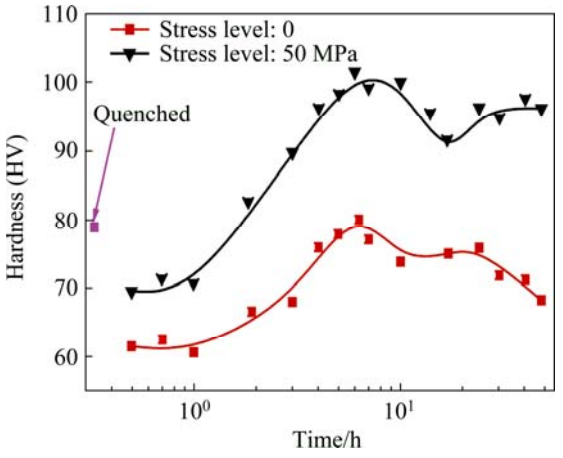

Fig. 2 Age-hardening curves of Al−5Cu alloy at 453 K

The TEM microstructure and the corresponding selected area electron diffraction patterns of θ'' phase for all samples in the peak-aging condition are shown in Fig. 3. Along the {100} zone axis of the electron beam,

the bright field image shows two "edge-on" {100} variants of the θ'' phase plates with the stress-free level (0). However, the external stress-aged (453 K, 50 MPa) sample obtained a stress-orientation precipitation phenomenon that only one variant of the θ'' phase plate is visible. It would be in an agreement with the previous work [16].

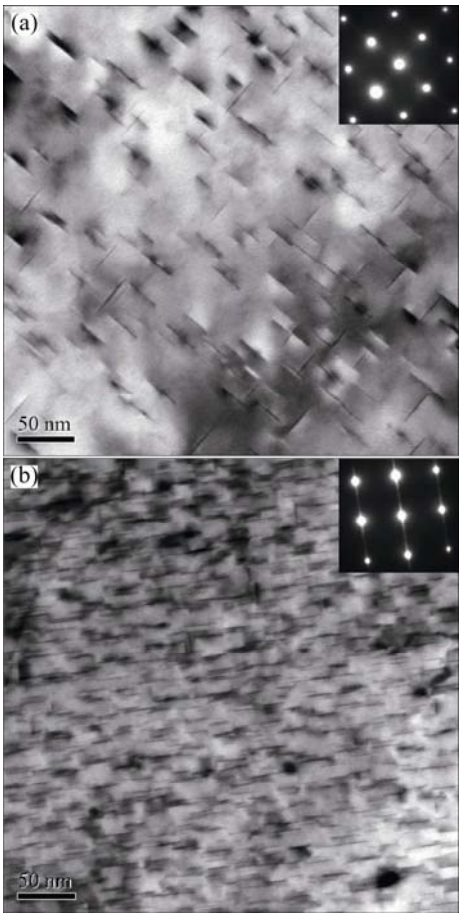

Fig. 3 TEM images of θ'' phase and its selected area electron diffraction patterns of alloy aged at 453 K for 6 h under 0 (a) and 50 MPa (b) external stress levels

It is clearly observed that the morphology of the θ'' phase under higher stress level is quite different that under the stress-free ones. The θ'' phase in higher stress-level (50 MPa) sample is finer than that in stress-free (0) aged sample; the volume fraction of the θ'' phase is higher than that in stress-free aging condition. So, the finer and more volume fraction θ'' phase under external stress contributed to the precipitation strengthening effect, resulting in the improvement of hardness.

Additionally, 4−6 bright-field TEM photographs (about 1000 θ'' phase plates counted) in peak-aging condition were used to make a precipitation phase length distribution statistics figure and evaluate the effect of external stress (0, 50 MPa) aging on the morphology of θ'' phase by quantitative method. The precipitation phase length distribution statistics is exhibited in Fig. 4. The average θ'' phase length under 50 MPa external stress level is determined as 19.83 nm while the result for stress-free aging is 28.79 nm. According to Fig. 4, external stress makes the θ'' phase plate length smaller, and the mode zone move from 30 nm to 20 nm in statistics distribution level. This implies that the external stress would promote the nucleation of θ'' phase, resulting in the formation of finer and more θ'' phase.

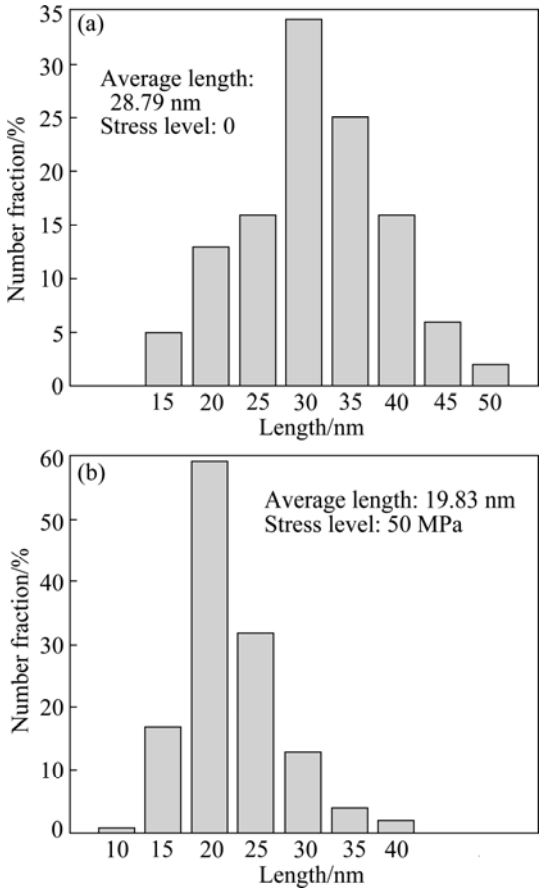

Fig. 4 θ'' phase plate length distribution (number fraction) counted by TEM images

3.2 θ'' phase precipitation behavior under external stress

The DSC (heat flow) curves under all different external stress levels at heating rate of 15 K/min are displayed in Fig. 5. The endothermic peak1 (peak 1a and peak 1b) and the exothermic peak 2 (peak 2a and peak 2b) correspond to the G.P. zone's dissolution period and the θ'' phase precipitation transformation, respectively, according to the work by HAYOUNE and HAMANA [19].

The exothermic peak 2b moves to the lower temperature since the precipitation behavior is influenced by the external-stress. Similarly, the endothermic peak1 shifts to the higher temperature because an amount of the G.P. zone is too little to detect in lower temperature. The θ'' phase precipitation rate results are shown in Fig. 6.

This supports the consideration that the sample under external stress has more amounts and quick precipitation of θ'' phase.

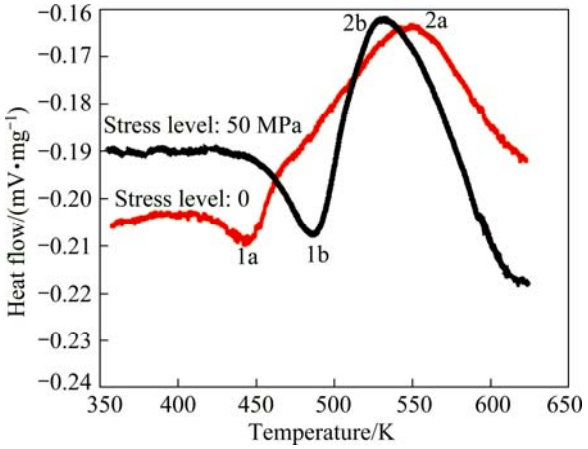

Fig. 5 DSC curves of samples at peak-aged condition under external stress

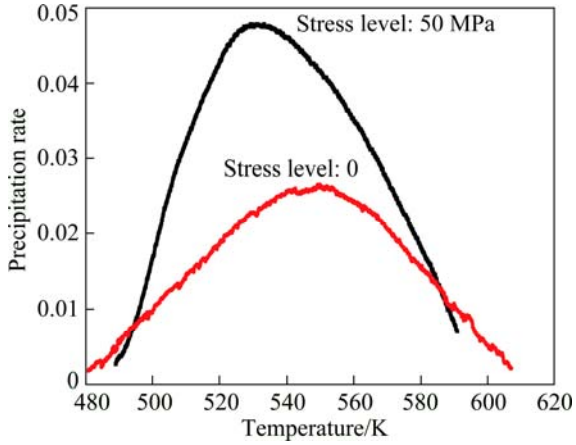

Fig. 6 Precipitation rate curves of samples under external stress

Furthermore, the apparent activation energy is determined according to the Kissinger method [20,21], as shown in Eq. (1), which can be used to evaluate the precipitation ability.

$$\ln\left(\frac{\beta}{T^2}\right)=-\frac{E_k}{R}\frac{1}{T}+C \tag{1}$$

where β is the heating rate; T is the temperature at the DSC heat flow curve peak; E_k is the activation energy; R is the gas constant; C is the integration constants.

With the different heating rates (β= 10, 15 and 20 K/min) and the peak (the exothermic peak 2) temperature T_p listed in Table 2, the scatter plot of $\ln(\beta/T_p^2)$ vs $(1/T_p)$ is shown in Fig. 7. The apparent activation energy under 50 MPa stress-aging is 90.1 kJ/mol and the activation energy is 99.2 kJ/mol in stress-free aging condition from Fig. 7, respectively. The apparent activation energy for the external stress aging is about 10% lower than that for the stress-free aging. It would be a strong evidence to show that the precipitation behavior is accelerated by external stress.

Table 2 Activation energies of θ'' phases obtained by Kissinger method

External stress/MPa	β/(K·min^{-1})	T_p/K	Activation energy/(kJ·mol^{-1})
0	10	540.1	99.2
	15	551.3	
	20	555.2	
50	10	519.1	90.1
	15	531.9	
	20	533.9	

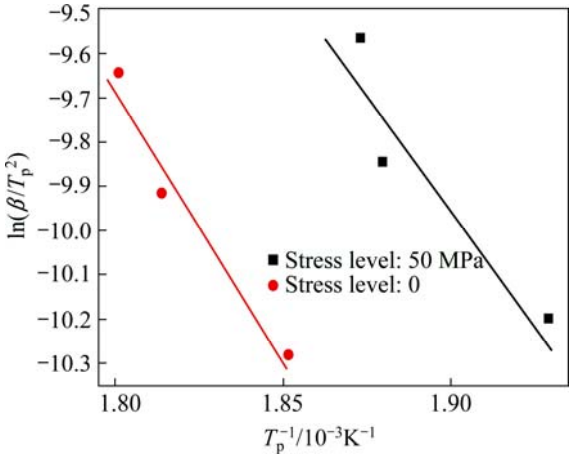

Fig. 7 Plots of $\ln(\beta/T_p^2)$ versus $1/T_p$ for θ'' phase precipitation under external stress

3.3 Interface energy and critical nucleation energy calculations under external stress aging

According to the classic nucleation theory, the driving force is the change of the system Gibbs free energy, and the main obstruction in this case is interface energy. The nucleation energy for age-hardening aluminum alloy could be determined according to Eq. (2):

$$W_r=\frac{4\pi}{3}r^3(\Delta E_{chem}+\Delta E_{strain})+4\pi r^2\gamma \tag{2}$$

where W_r is the nucleation energy; r is the nucleation radius; ΔE_{chem} is the chemical potential; ΔE_{strain} is the strain energy; γ is the interface energy between precipitation phase and the matrix. And the critical nucleation energy could be expressed as Eq. (3) when the critical nucleation radius r^* is determined.

$$W_r(r^*)=\frac{16\pi}{3}\frac{\gamma^3}{(\Delta F_{chem}+\Delta F_{elastic})^2} \tag{3}$$

The chemical potential change (ΔE_{chem}) under

external stress (transforming into strain (ε)) can be obtained by Eq. (4) according to the work of RAVI et al [22] where the μ is the chemical potential. And the results are listed in Table 3 according to the first principle calculation method. The change in chemical potential is not apparent according to the calculation results.

$$\Delta E_{\text{chem}}(\varepsilon) = \mu(\text{Al}_3\text{Cu}(\varepsilon)) + (31-3)\mu(\text{Al}(\varepsilon)) - \mu(\text{Al}_{31}\text{Cu}(\varepsilon)) \quad (4)$$

Table 3 Results of chemical potential and chemical potential change

External strain/ stress level	$\mu(Al_3Cu)$/ eV	$\mu(Al)$/ eV	$\mu(Al_{31}Cu)$/ eV	$\Delta E_{chem}(\varepsilon)$/ eV
0	−30.6519	−3.7446	−119.9346	−15.5671
0.002	−30.6518	−3.7445	−119.9315	−15.5662
0.004	−30.6517	−3.7441	−119.9194	−15.5665
0.006	−30.6512	−3.7434	−119.8985	−15.5678

The change of the elastic strain energy (ΔE_{strain}) could be described by the Eshelby's elastic inclusion model [23] and the mathematic expression is shown as Eq. (5).

$$\Delta E_{\text{strain}} = -E\delta^2 \quad (5)$$

Under stress-free aging condition, the misfit δ could be determined as −0.052 between θ'' phase [24] and matrix, the calculated elastic modulus is 77 GPa. However, the misfit δ was determined to be −0.058 under 50 MPa external stress. Therefore, the elastic strain energy would be similar for the all external stress levels (0, 50 MPa) to some extent. This means that lower external stress level has little influence on the strain energy.

The interface energy can be expressed as Eq. (6).

$$\gamma_{\text{interface}}(\varepsilon) = \frac{1}{2A}[E_0(\varepsilon) - N_{\text{Al}}\mu_{\text{Al}}(\varepsilon) - N_{\text{Cu}}\mu_{\text{Cu}}(\varepsilon)] = \frac{1}{2A}\{E_0(\varepsilon) - N_{\text{Al}}\mu_{\text{Al}}(\varepsilon) - \frac{1}{3}N_{\text{Al in Al}_3\text{Cu}}\mu_{\text{Al}_3\text{Cu}}(\varepsilon) - (N_{\text{Cu in Al}_3\text{Cu}} - \frac{1}{3}N_{\text{Al in Al}_3\text{Cu}})[\mu_{\text{Cu}}(\varepsilon) + KT\ln\alpha_{\text{Cu in Al}}]\} \quad (6)$$

where A is the area defined in the interface model; E_0 is the total energy of interface model; μ_i and N_i are the chemical potential and the atom number of species i, respectively; ε is the applied strain under external stress; $\alpha_{\text{Cu in Al}}$ is the activity of Cu in Al matrix; $\alpha_{\text{Cu in Al}}$ can be determined as shown in Fig.8 according to Ref. [25].

The interface energy is calculated by the first principle calculation (VASP software packages), and the interface energy results in different strains are shown in Fig. 9. The results show that the interface energy decreases gradually by the effect of the external stress/strain from 0.88 J/m^2 to 0.82 J/m^2. As a result, the influence of external stress is more significant on the interface energy than on the chemical potential and the elastic strain energy. When the aging temperature is 453 K, the critical nucleation energy under 50 MPa external stress level is 19 % lower than that under level 0 according to Eq. (3). And the precipitation behavior under external stress could be stimulated as the nucleation energy becomes low. The θ'' precipitation phase would be finer and the precipitation processing would be easier, which is supported by the experiment results.

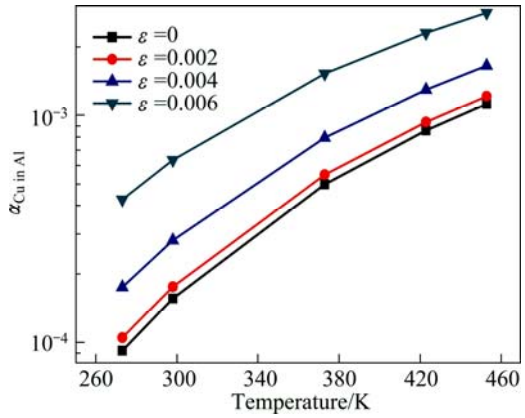

Fig. 8 Calculated activity α_{Cu} in Al under different strain/stress levels

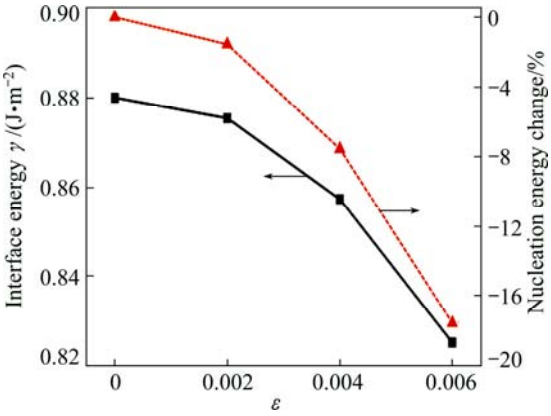

Fig. 9 Calculated interface energy and nucleation energy change in all strain/stress levels

In addition, it is implied that the interface energy is the major factor to influence the nucleation processing. The change of the critical nucleation energy is larger than that of the apparent precipitation activation energy since the effect of the external stress would be different during the coarsening processing of precipitation.

4 Conclusions

1) The applied external stress contributes to the

improvement of hardness of Al−Cu alloy. The size of θ'' phase under 453 K, 6 h, 50 MPa stress aging is 19.83 nm, which is smaller than that of the θ'' phase (28.79 nm) in stress-free condition (453 K, 6 h).

2) The precipitation process of θ'' phase is accelerated by external stress aging according to the shift of the DSC heat flow exothermic peak. And the precipitation under 50 MPa stress is dramatically accelerated compared with the stress-free aged one. The apparent activation energy for the external stress-aging is 90.02 kJ/mol, 10% lower than that for stress-free aging.

3) The first principle calculation results show that the external stress has an obvious influence on the interface energy. The interface energy under external stress condition is 0.82 J/m^2, 6% lower than the interface energy (0.88 J/m^2) in stress-free aging condition. The critical nucleation energy is 19% lower than that in stress-free aging condition. The change of nucleation energy determines the precipitation behavior and morphology of θ'' phase.

Acknowledgements

This paper was supported by the High Performance Computing Center of Central South University, China.

References

[1] SMALLMAN R E, BISHOP R J. Modern physical metallurgy and materials engineering: Science, process applications [M]. 6th ed. Butterworth-Heinemann Press, 1999.

[2] SON S K, TAKEDA M, MITOME M, BANDO Y, ENDO T. Precipitation behavior of an Al−Cu alloy during isothermal aging at low temperatures [J]. Material Letter, 2005, 59(6): 629−632.

[3] JANG J H, NAM D G, PARK Y H, PARK I M. Effect of solution treatment and artificial aging on microstructure and mechanical properties of Al−Cu alloy [J]. Transactions of Nonferrous Metals Society of China, 2013, 23(3): 631−635.

[4] XU Guo-fu, PENG Xiao-yan, LIANG Xiao-peng, LI Xu, YIN Zhi-min. Constitutive relationship for high temperature deformation of Al−3Cu−0.5Sc alloy [J]. Transactions of Nonferrous Metals Society of China, 2013, 23(3): 1549−1555.

[5] SILCOCK J M, HEAL T J, HARDY H K. Structural aging characteristics of binary aluminum−copper alloys [J]. Journal of the Institute of Metals, 1954, 82: 239−248.

[6] LOECHTE L, GITT A, GOTTSTEIN G, HURTADO I. Simulation of the evolution of GP zones in Al−Cu alloys: An extended Cahn–Hilliard approach [J]. Acta Materialia, 2000, 48(11): 2969−2984.

[7] BOURGEOIS L, DWYER C, WEYLAND M, NIE J F. The magic thicknesses of theta' precipitates in Sn-microalloyed Al−Cu [J]. Acta Materialia, 2011, 60(2): 633−644.

[8] RINGER S P, SAKURAI T, POLMEAR I J. Origins of hardening in aged Al−Cu−Mg−(Ag) alloys [J]. Acta Materialia, 1997, 45(9): 3731−3744.

[9] CHEN Z G, ZHENG Z Q. Microstructural evolution and ageing behaviour of the low Cu−Mg ratio Al−Cu−Mg alloys containing scandium and lithium [J]. Scripta Materialia, 2004, 50: 1067−1071.

[10] XU G F, ZHOU M S, YIN Z M. Effects of Sc addition on age-hardening and precipitation behavior of Al−3.0% Cu alloy [J]. Mining and Metallurgical Engineering, 2006, 26(2): 92−95, 99.

[11] ZHU A W, STARKE E A. Materials aspects of age-forming of Al−*X*Cu alloys [J]. Journal of Materials Processing Technology, 2001, 117(3): 354−358.

[12] OBLAK J M, PAULONIS D F, DUVALL D S. Coherency strengthening in Ni base alloys hardened by DO_{22} γ' precipitates [J]. Metallurgical Transactions, 1974, 5(1): 143−153.

[13] LOUTHAN M R, ANGERMAN C L. Thermo-mechanical effects on hydride precipitation in zircaloy-2 [J]. Metallurgical Transactions, 1973, 4(7): 1763−1765.

[14] HOSFORD W F, AGRAWAL S P. Effect of stress during aging on the precipitation of θ' in Al-wt pct Cu [J]. Metallurgical and Materials Transactions A, 1975, 6(3): 487−491.

[15] CHEN Da-qin, ZHENG Zi-qiao, LI Shi-chen, CHEN Zhi-guo. Mechanism of stress aging in Al−Cu(−Mg−Ag) alloys [J]. Transactions of Nonferrous Metals Society of China, 2004, 14(4): 779−784.

[16] ZHU A W, STARKE E A. Stress aging of Al−*x*Cu alloys experiments [J]. Acta Materialia, 2001, 49(12): 2285−2295.

[17] LAN G Q, JIANG Y, YI D Q, LIU S J. Theoretical prediction of impurity effects on the internally oxidized metal/oxide interface: The case study of S on Cu/Al_2O_3 [J]. Physical Chemistry Chemical Physics, 2012,14: 11178−11184.

[18] KRESSE G, FURTHMÜLLER J. VASP the guide [EB/OL]. http://cms.mpi.univie.ac.at/vasp/vasp/ vasp.html. 2013.

[19] HAYOUNE A, HAMANA D. Structural evolution during non-isothermal ageing of a dilute Al−Cu alloy by dilatometric analysis [J]. Journal of Alloys and Compounds, 2009, 474(1−2): 118−123.

[20] GHOSH K S, GAO N. Determination of kinetic parameters from calorimetric study of solid state reactions in 7150 Al−Zn−Mg alloy [J]. Transactions of Nonferrous Metals Society of China, 2011, 21(6): 1199−1209.

[21] LI Hai, WANG Xiu-li, SHI Zhi-xin, WANG Zhi-xiu, ZHENG Zi-qiao. Precipitation behaviors of Al−Mg−Si−(Cu) aluminum alloys during continuous heating [J]. The Chinese Journal of Nonferrous Metals, 2011, 21(9): 2028−2034. (in Chinese)

[22] RAVI C, WOLVERTON C, OZOLIŅŠ V. Predicting metastable phase boundaries in Al−Cu alloys from first-principles calculations of free energies: The role of atomic viberations [J]. Europhysics Letters, 2006, 73(5): 719−725.

[23] WANG Hong-wei, YI dan-qing, CAI Jin-ling, WANG Bin. Effect of stress aging on mechanical properties and microstructures of 2E12 aluminum alloy [J]. The Chinese Journal of Nonferrous Metals, 2011, 21(12): 3019−3025. (in Chinese)

[24] SKROTZKI B, SHIFLET G J, STARKE E A. On the effect of stress on nucleation and growth of precipitates in an Al−Cu−Mg−Ag alloy [J]. Metallurgical and Materials Transactions A, 1996, 27: 3431−3444.

[25] JIANG Y, SMITH J R, EVANS A G. Temperature dependence of the activity of Al in dilute Ni(Al) solid solutions [J]. Physical Review B, 2006, 74: 224110.

外场应力对 Al−Cu 合金中 θ''相形貌及析出行为的影响

傅 上[1,2]，易丹青[1,2]，刘会群[1,2]，江 勇[1,2]，王 斌[1,2]，胡 湛[1,2]

1. 中南大学 材料科学与工程学院，长沙 410083；
2. 中南大学有色金属材料科学与工程教育部重点实验室，长沙 410083

摘 要：对 Al−5Cu 铝合金在时效过程中施加弹性加载，并采取透射电镜、热分析研究外应力时效作用下 θ''析出相的形态和析出行为。结果表明：在 50 MPa 的外力作用下，在 453 K 时效 6 h 后的析出相尺寸是 19.83 nm，小于其常规时效(453 K，6 h)的尺寸 28.79 nm。热分析结果揭示施加应力后时效析出过程得到促进，同时析出激活能结果表明外应力作用使得激活能下降 10%。第一性原理计算结果发现，外应力作用使得析出相与基体的界面能下降 6 %；结合经典形核相变理论分析讨论，临界形核功受到外应力作用下降 19 %，从而引起了析出相形态和析出行为的改变。

关键词：Al−Cu 合金；应力时效；形态；析出行为；第一原理计算；界面能

(Edited by Hua YANG)